16th World Conference on Earthquake, 16WCEE 2017

Santiago Chile, January 9th to 13th 2017

Paper N° 1033

Registration Code: S-F1461770147

INFLUENCE OF CYCLIC DEGRADATION ON INELASTIC SEISMIC DEMANDS IN STEEL MOMENT FRAMES

M.A Bravo-Haro [(1)], A. Tsitos [(2)], A.Y. Elghazouli [(3)]

[(1)] Ph.D. Student, Dept. of Civil and Environmental Engineering, Imperial College London, UK, miguel.bravo-haro14@imperial.ac.uk
[(2)] Research Associate, Dept. of Civil and Environmental Engineering, Imperial College London, UK, a.tsitos@imperial.ac.uk
[(3)] Professor, Dept. of Civil and Environmental Engineering, Imperial College London, UK, a.elghazouli@imperial.ac.uk

Abstract

This paper assesses the influence of the cyclic strength and stiffness degradation on the global and local inter-storey drift demands in moment resistant steel frames (MRF) designed according to Eurocode 8. The underlying question that motivated this research is whether refined structural modelling techniques such as those able to simulate steel degradation phenomena are relevant at the most typical design level, in order to satisfy the No-Collapse requirements imposed by the seismic code. For this purpose a set of low-rise and mid-rise MRFs, designed to European guidelines, were subjected to incremental dynamic analyses (IDA) using a suite of 56 far-field ground motion records. Two main modelling approaches were considered: (i) distributed plasticity modelling with fibre sections and elasto-plastic hardening material, and (ii) concentrated plasticity modelling with plastic hinges characterized by a constitutive model that includes deterioration effects. The results obtained from this set of analysis suggest that in the case of low-rise frames, cyclic degradation does not significantly affect the structural response, measured in terms of inter-storey drifts, while in the case of medium-rise frames degradation modelling is more relevant, resulting in up to 40% higher inter-storey drifts values. It is concluded, based on the findings of this study, that detailed assessments would be required in order to quantify the influence of cyclic degradation modelling in the structural response of medium-rise moment frame with various typologies.

Keywords: steel moment frames; seismic design; Eurocode 8; displacement demands; deterioration modelling; cyclic degradation.

1. Introduction

In performance-based earthquake engineering, building structures are evaluated based on predefined performance objectives for a given seismic hazard scenario. These performance levels correspond to structural behaviour ranging from elastic up to structural collapse. The fact that nowadays engineers have access to ever more powerful computing systems, has enabled the assessment of the dynamic behaviour of structures well into the nonlinear domain and the detailed examination of structural collapse aspects. Consequently, structural behaviour can be assessed at an ultimate level, where the seismic drift demands on buildings may be significantly influenced by considerations such as P-Δ effects or amplified by strength and stiffness deterioration of structural components. A comprehensive account of these aspects is presented in FEMA P695 [1] in which a methodology is presented for the estimation of the collapse probability using the structural response at the code-defined maximum considered earthquake (MCE) as a benchmark, and introducing the concept of collapse margin ratio (CMR). The latter can be defined as the amount by which the MCE spectral acceleration at the main period of the system must be multiplied by in order to achieve building collapse for 50% of the ground motions used in the analysis. This methodology intends to supplement the current seismic codes in extreme situations where large levels of inelasticity would be expected. However, up to the design seismic action provided by the codes (usually through a design response spectrum), where the structure has a low likelihood of collapse, simplified analysis procedures are applicable [1].

Based on the above considerations, the main objective of this paper is to appraise the global and storey drift demands in moment resisting frames which are designed to comply with Eurocode 8 (EC8) [2] through utilization of both: (i) distributed-plasticity modelling without deterioration, and (ii) concentrated (lumped) plasticity modelling able to take into account degradation phenomena, and consequently evaluate their suitability for the performance objectives required by EC8. To this end, a set of 54 frames is subjected to nonlinear static pushover analyses and to dynamic time-history analyses using a suite of 56 far-field ground motions, which are scaled in order to correspond to four distinct levels of inelasticity, quantified by the "behaviour" factor q'.

2. Background on inelastic drift demands

The reliable determination of inelastic structural displacements under seismic loading is a key consideration in performance-based design. Consequently, numerous assessment methodologies have been proposed, founded on basic principles [3], or using sophisticated non-linear response history analyses (NRHA) [4], [5], [6], [7], [8] as well as alternative approaches based on dimensional analysis [9]. Despite the computational burden of NRHA, they are increasingly utilized in the seismic design and assessment of buildings, due to the rapid increase in computational power and accessibility of cloud-based distributed computing clusters. However, the dissemination of cutting-edge modelling techniques clearly needs to be coupled with expertise that is required from the designer [10], [11].

Most of the available expressions for inelastic displacement estimation are based on simplified relationships between elastic and inelastic drifts such as the equal displacement rule [1], [12]. Numerous studies based on multi-degree of freedom (MDOF) models have proposed prediction methods for inelastic drift demands [7], [8]. However, in most cases, they have not taken into account the strength and stiffness degradation of the main structural components (e.g. beams and columns) for estimating peak displacements with NRHA. The need for hysteretic models with degradation is evident in the case of excessive levels of deformation demand in structural members, where locally initiated damage triggers strength and stiffness deterioration, eventually leading to a significant reduction of the global structural integrity [13]. Because of this, the deterioration modelling approach is important for the study of structural collapse phenomena. Consequently, the need for reliable prediction of the structural collapse potential of new and existing buildings has motivated studies on the assessing and quantifying deformation capacity and degradation rates of dissipative steel elements [14], [15], [16]. Based on the above discussion, a question arises on the relevance of hysteretic modelling with degradation for predicting inelastic displacements of code-designed MRFs. The two fundamental seismic design levels considered in EC8 Part 1 are 'No-Collapse' and 'Damage-Limitation', which broadly refer to ultimate and serviceability limit states, respectively. On the one hand, the capacity design is more closely associated with large events ('No-Collapse'). However, several verifications are also required to ensure compliance with serviceability limits.

In light of the above discussion, the objective of this paper is twofold. First, to assess the influence of hysteretic degradation modelling on inelastic displacement prediction for steel MRFs and, second, to compare the lumped plasticity modelling approach against the distributed plasticity method at levels of seismic displacement demand typically observed in MRFs, corresponding to ductility demands ranging from 3 to 6 according to a methodology presented in Section 4.

3. Structural configurations & ground motions

3.1 Frame characteristics and modelling assumptions

To assess global and storey inelastic drift demands, a large set of 54 moment frames that satisfy the design provisions of Eurocode 3 (EC3) [17] and EC8 [2] was considered. The set consisted of typologies of 3, 5 and 7-storey moment resisting frames which were used in previous studies by Kumar et al. [8] and which were also supplemented by a subset of 9-storey structures that was added in order to cover a wider range of structural parameters (see Table 1). More specifically, the full set of moment frames comprised total heights between 11.5 m and 32.5 m, whereas the range of fundamental periods (T_1) obtained using eigenvalue analysis incorporated values from 0.4 s up to 1.85 s.

Fig. 1 presents plan and elevation views of the typical structural system, consisting of 3 lateral load resisting frames with a span of 6 m and storey height of 4.5 m and 3.5 m, for the first and upper storeys, respectively. The orthogonal direction was considered to have an independent lateral load resisting system. Therefore, the moment frames were assumed two-dimensional. Initially, the interior moment frames considered in this study were designed for resisting gravity loads according to EC3 requirements. Dead loads of 5.75 kN/m^2 and 4.75 kN/m^2, and live loads of 2 kN/m^2 and 1 kN/m^2, were applied to the typical floors and the roof, respectively. Seismic design was then performed following the requirements assuming various cases of seismic hazard (further details are given by Kumar et al. [8]). Since the structures satisfy EC8 regularity conditions, the lateral force method of analysis was used at the design stage, with an equivalent lateral seismic loading based on the fundamental mode shape. Table 1 presents a summary of the selected cross-sections for the additional 9-storey sub-set, as well as the fundamental period, the over-strength due to redistribution α (defined as the ratio α_u/α_1 in EC8), and the mass participation factor γ of the first mode. (The labels used for the frame typologies start with the letters A, B, C and D that correspond to the 3, 5, 7 and 9-storey variations, respectively).

Table 1 - Design details and corresponding structural characteristics of the 9-storey frames

Frame	Design details		Structural properties		
ID	Beams	Columns	T1, s	α	γ
D01	IPE600, IPE600, IPE600, IPE600, IPE600, IPE600, IPE600, IPE550, IPE550	HEM700, HEM650, HEM650, HEM650, HEM650, HEM650, HEM600, HEM600, HEM600	1.04	1.36	0.82
D02	IPE550, IPE550, IPE550, IPE550, IPE550, IPE500, IPE500, IPE450, IPE450	HEM600, HEM600, HEM600, HEM600, HEM550, HEM550, HEM550, HEM500, HEM500	1.23	1.34	0.81
D03	IPE550, IPE550, IPE550, IPE500, IPE500, IPE500, IPE450, IPE450, IPE450	HEM600, HEM600, HEM550, HEM550, HEM550, HEM550, HEM550, HEM500, HEM450	1.28	1.33	0.79
D04	IPE550, IPE550, IPE550, IPE500, IPE500, IPE450, IPE450, IPE400, IPE360	HEM550, HEM550, HEM500, HEM500, HEM500, HEM450, HEM450, HEM400, HEM400	1.35	1.27	0.78
D05	IPE500, IPE500, IPE500, IPE500, IPE500, IPE450, IPE450, IPE400, IPE360	HEM500, HEM500, HEM500, HEM450, HEM450, HEM450, HEM400, HEM400, HEM400	1.47	1.30	0.80
D06	IPE450, IPE450, IPE450, IPE450, IPE450, IPE400, IPE400, IPE400, IPE360	HEM450, HEM450, HEM450, HEM400, HEM400, HEM400, HEM400, HEM400, HEM360	1.74	1.42	0.80
D07	IPE450, IPE450, IPE450, IPE450, IPE450, IPE400, IPE400, IPE400, IPE360	HEM450, HEM450, HEM360, HEM360, HEM360, HEM360, HEM360, HEM360, HEM360	1.77	1.27	0.80
D08	IPE750x137, IPE750x137, IPE750x137, IPE600, IPE600, IPE600, IPE500, IPE500, IPE360	HEM800, HEM800, HEM800, HEM700, HEM700, HEM700, HEM600, HEM600, HEM500	0.92	1.24	0.76
D09	IPE500, IPE500, IPE500, IPE500, IPE500, IPE500, IPE500, IPE500, IPE400	HEB450, HEB450, HEB450, HEB400, HEB400, HEB400, HEB400, HEB400, HEB300	1.63	1.15	0.84
D10	IPE550, IPE550, IPE550, IPE500, IPE500, IPE500, IPE500, IPE500, IPE450	HEM600, HEM600, HEM600, HEM600, HEM600, HEM550, HEM550, HEM500, HEM450	1.27	1.35	0.80
D11	IPE750x137, IPE600, IPE600, IPE600, IPE600, IPE600, IPE500, IPE500, IPE450	HEM800, HEM800, HEM800, HEM700, HEM700, HEM600, HEM550, HEM500, HEM450	0.99	1.35	0.77
D12	IPE600, IPE600, IPE600, IPE600, IPE600, IPE600, IPE500, IPE500, IPE400	HEM700, HEM700, HEM700, HEM700, HEM700, HEM700, HEM600, HEM600, HEM400	1.04	1.33	0.81
D13	IPE450, IPE450, IPE450, IPE450, IPE450, IPE450, IPE400, IPE400, IPE360	HEB500, HEB500, HEB500, HEB400, HEB400, HEB360, HEB360, HEB360, HEB360	1.81	1.32	0.81
D14	IPE450, IPE450, IPE450, IPE450, IPE450, IPE400, IPE400, IPE400, IPE360	HEB500, HEB500, HEB500, HEB360, HEB360, HEB360, HEB360, HEB360, HEB360	1.85	1.27	0.79
D15	IPE550, IPE550, IPE550, IPE500, IPE500, IPE500, IPE450, IPE400, IPE360	HEM550, HEM550, HEM550, HEM500, HEM500, HEM450, HEM450, HEM400, HEM400	1.34	1.27	0.79

The distributed plasticity approach with fibre sections was used as a benchmark, taking into account that this modelling type has been widely used and calibrated against experimental tests. Consequently, it does not require particular tuning or modifications for performing NRHA [10], fundamentally because there is a direct physical basis in the fibre discretisation of the section and the gradual spread of plasticity along the structural members. The beams and columns are modelled in OpenSees [18] using non-linear force-based elements with seven-point Gauss-Lobatto integration points and each section was discretised in 48 fibres (see Fig. 1(a)). A bilinear stress-strain model for steel was adopted with a post-yield stiffness ratio of 0.5%. No deterioration was considered at the material level. Distributed plasticity models are not significantly influenced by the type of damping employed even at highly inelastic levels [10], hence standard Rayleigh-type damping based on initial stiffness was used in this case, assuming 2% of modal damping ratio for the first and third modal frequencies.

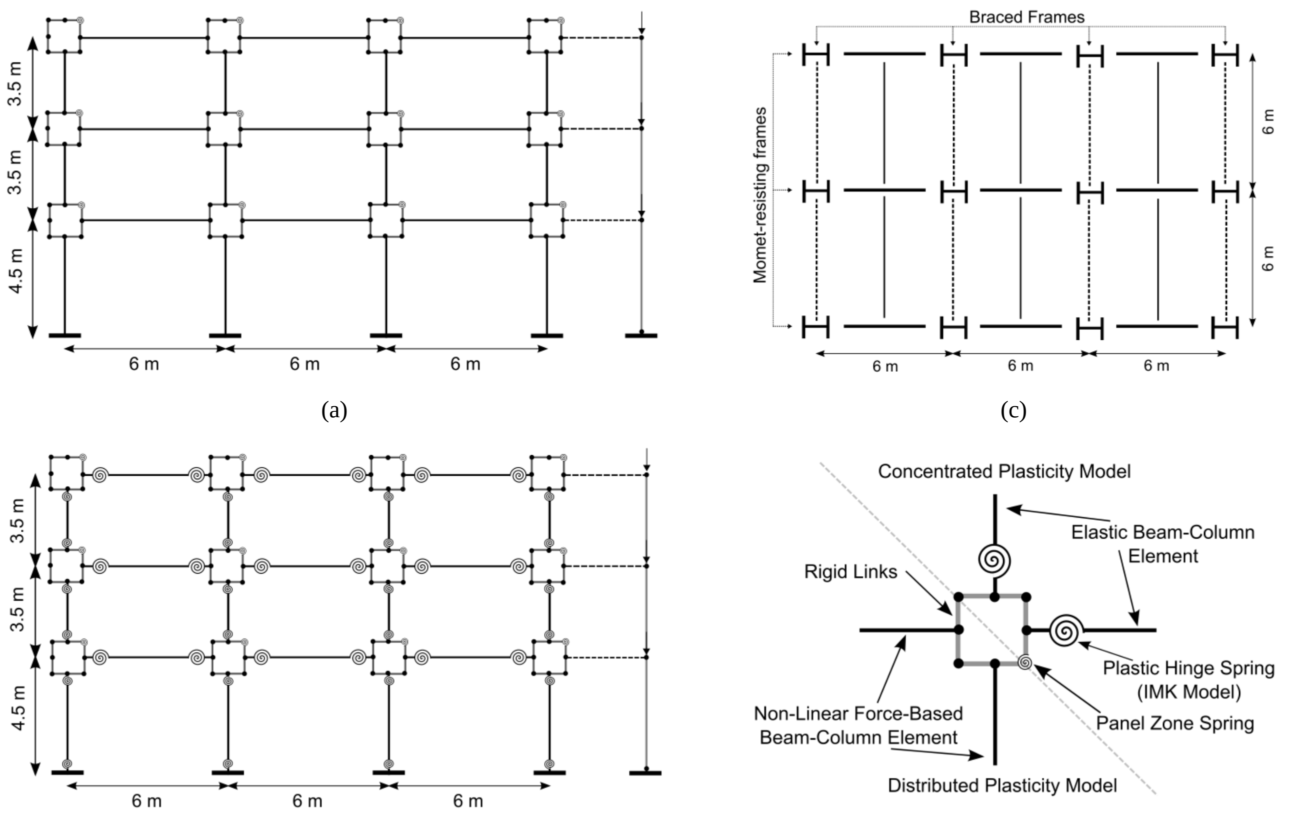

Fig. 1 – Typical frame elevations for models with: (a) distributed plasticity and (b) concentrated plasticity. Plan view of MRFs typology (c) and connection region modelling detail (d), for both modelling approaches.

On the other hand, concentrated plasticity models followed a typical modelling strategy, in which each beam and column comprised three distinct members in series, i.e. two rotational springs (zero-length elements) at the ends and an elastic beam element in the middle (see Fig. 1(b)). A description of the inelastic behaviour of each component can be found in the PEER/ATC-72 [19]particularly concerning the multi-linear moment-rotation curve that defines the rotational spring. The constitutive law of the moment-rotation interaction curve assigned to the beams is based on the modified Ibarra-Medina-Krawinkler (IMK) deterioration model [20] whose input parameters have been calibrated by Lignos and Krawinkler [13],[15] through extensive multivariate regression analysis, based on a large experimental database. It is worth mentioning that the database of steel profiles used for the estimation and calibration of key parameters of the IMK model, mainly consists of experiments with US steel profiles, while limited information exists for European steel profiles at present [16].

The lumped plasticity approach used for beams, which ignores the effect of axial load in the member, was also used in the columns along the height of the frames, following the recommendation in PEER/ATC-72, in the case of "low" axial loads at the base level (i.e. a value of the ratio of axial load to the yield strength of the section in compression: $P/P_y < 0.2$) [19]. The influence of the reduction of the bending capacity at the base columns due to interaction with axial load was determined to be insignificant for the frame typologies examined in this paper. The method proposed by Zareian and Medina [21] was adopted for modelling of structural damping. No damping was assigned to the nonlinear springs, and the local stiffness matrix of the elastic beam-column elements was appropriately tuned (increase of the stiffness) by means of the elastic elements with stiffness modifiers available in the OpenSees platform. Rayleigh-type damping based on the initial modified stiffness matrix was applied to the non-linear beams/columns, assuming a damping ratio of 2% at the first and third modal frequencies.

The strength and deformability of the column web panel zone region was simulated (in both modelling approaches) according to the widely adopted model proposed by Krawinkler et al. [22], using a parallelogram assembly of pinned rigid elements (Fig. 1(d)). A tri-linear moment-rotation spring was located at one corner of the parallelogram and simulated the non-linear response of the panel zones, considering both the column web panel uniform yielding mechanism and the subsequent plastic hinging at the column flanges or the continuity plates.

3.2 Ground motion records and scaling approaches

The ground-motion records used for the NRHA were a subset of the PEER NGA strong-motion database [23] comprising only far-field records. The set included strong-motion records with PGA higher than 0.2 g and PGV higher than 20 cm/s from most large-magnitude events in the database ($M > 6.5$), a range of distances from the fault from 8.7 km up to 160 km and from recording sites with soil type characterised as A, B and C according to the NEHRP soil classification. Table 2 summarises the 28 individual earthquake events along with their main characteristics in terms of magnitude, M, fault mechanism and mean period, T_m, for each horizontal component. Fig. 2 shows the 56 individual acceleration response spectra (i.e. 28 records, 2 directional components each) along with the median spectrum. It has been demonstrated in previous studies [8], [24] [25] that the mean period, T_m, has a significant effect on inelastic drifts demands and therefore this ground motion characteristic was also considered in this paper, in order to produce comparable results.

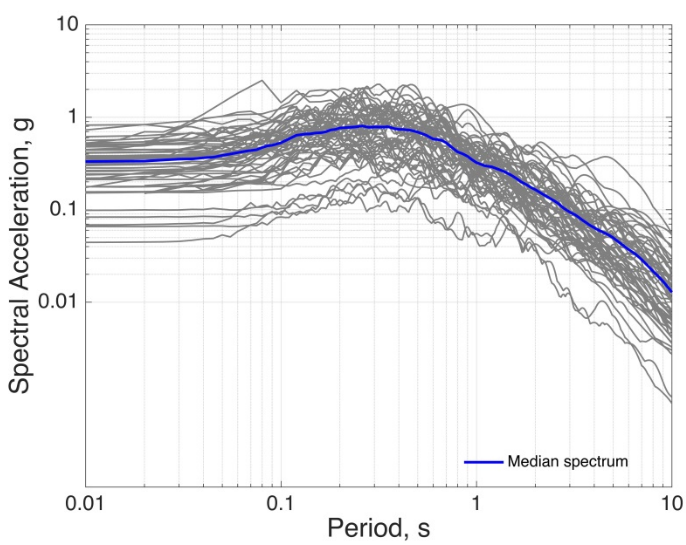

Fig. 2 – Acceleration response spectra of the ground motion record set and median spectrum

Table 2 - Catalogue of earthquakes used in the study and seismological characteristics (Fault Mechanism: RV = reverse, SS = strike slip and RO = reverse oblique)

Earthquake name	M	Mechanism	Tm, s	Earthquake name	M	Mechanism	Tm, s
Chi-Chi, Taiwan 1999-09-20	7.62	RO	0.96, 1.05	Cape Mendocino 1992-04-25	7.01	RV	0.44, 0.54
Chi-Chi, Taiwan 1999-09-20	7.62	RO	0.53, 0.47	Loma Prieta 1989-10-18	6.93	RO	0.49, 0.49
St Elias, Alaska 1979-02-28	7.54	RV	2.02, 1.91	Loma Prieta 1989-10-18	6.93	RO	0.62, 0.37
St Elias, Alaska 1979-02-28	7.54	RV	1.44, 1.10	Kobe, Japan 1995-01-16	6.90	SS	0.53, 0.49
Kocaeli, Turkey 1999-08-17	7.51	SS	0.89, 1.05	Kobe, Japan 1995-01-16	6.90	SS	0.73, 0.76
Kocaeli, Turkey 1999-08-17	7.51	SS	0.63, 0.31	Northridge-01 1994-01-17	6.69	RV	0.33, 0.32
Manjil, Iran 1990-06-20	7.37	SS	0.32, 0.32	Northridge-01 1994-01-17	6.69	RV	0.56, 0.60
Kern County 1952-07-21	7.36	RV	0.54, 0.55	San Fernando 1971-02-09	6.61	RV	0.36, 0.56
Landers 1992-06-28	7.28	SS	0.66, 0.91	Superstition Hills-02 1987-11-24	6.54	SS	0.94, 0.65
Landers 1992-06-28	7.28	SS	0.56, 0.42	Superstition Hills-02 1987-11-24	6.54	SS	0.48, 0.49
Duzce, Turkey 1999-11-12	7.14	SS	0.78, 0.55	Imperial Valley-06 1979-10-15	6.53	SS	0.68, 0.62
Hector Mine 1999-10-16	7.13	SS	0.64, 0.79	Imperial Valley-06 1979-10-15	6.53	SS	0.42, 0.45
Hector Mine 1999-10-16	7.13	SS	0.63, 0.61	Borrego 1942-10-21	6.50	SS	0.58, 0.54
Cape Mendocino 1992-04-25	7.01	RV	1.09, 0.75	Friuli, Italy-01 1976-05-06	6.50	RV	0.51, 0.40

4. Assessment of seismic drift demands

4.1 Numerical procedures

Initially, in order to compare distributed and lumped plasticity approaches, incremental dynamic analysis (IDA) was performed on four frame cases - including one per subset, namely A03, B15, C08, and D01, with 3, 5, 7 and 9 storeys, respectively. In total, 1792 NRHA cases were run both for distributed plasticity as well as lumped plasticity models with cyclic degradation, as described above. The analyses were carried out by scaling the records with respect to the spectral acceleration at the fundamental period, T_1, in order to attain four different levels of relative intensity, q', emulating the behaviour factor, q, in EC8. The scaling factor, S_F, for each individual record in order to attain a target intensity factor, q', was determined as follows:

$$S_F = q' \cdot \frac{V_1}{S_a\,(T_1) \cdot m \cdot \gamma} \tag{1}$$

where $S_a(T_1)$ corresponds to the spectral acceleration of a given record at the fundamental period of the frame, V_1 is the base shear at the moment of formation of first plastic hinge in the frame (obtained from a first-mode force profile static pushover analysis), m is the seismic mass and γ represents the effective mass participation ratio of the first mode. Four inelasticity levels were assumed for each ground motion record (q' =3, 4, 5 and 6) and in order to produce the database for the inelastic drift estimation, the maximum roof displacement (Δ_{max}) and the maximum inter-storey drift (θ_{max}) were recorded and finally post-processed for obtaining the global drift modification factor, δ_{mod}, and the inter-storey drift modification factor, θ_{mod}. The modification factors are defined as follows:

- The global drift modification factor, δ_{mod}, is the ratio of the maximum roof displacement, Δ_{max}, obtained from NRHA, for a given intensity q', to the product of q' and the roof displacement at first yield, $\Delta_{1,roof}$, as obtained from a pushover analysis with a "first-mode" lateral force profile:

$$\delta_{mod} = \frac{\Delta_{max}}{q' \cdot \Delta_{1,roof}} \tag{2}$$

- The maximum inter-storey drift modification factor, θ_{mod}, is defined similarly to δ_{mod} , but using the maximum inter-storey drift, θ_{max}, and the maximum inter-storey drift at first yield, $\theta_{1,max}$, which may occur at different storeys:

$$\theta_{mod} = \frac{\theta_{max}}{q' \cdot \theta_{1,max}} \tag{3}$$

In the following sections, summary results from pushover analyses for the 3 and the 9-storey frame set are presented, followed by the results of the IDA at the various intensity levels, q', for 4 frame typologies, in terms of the displacement modification factors defined above.

4.2 Pushover analyses

The global pushover curves, calculated from non-linear static analyses of the 54 frames with a lateral force profile based on the modal shape of the first mode, offer a significant insight into the structural behaviour. Summary results for the case of frames modelled according to the concentrated plasticity approach with IMK plastic hinges are presented in this section. Fig. 3 depicts the pushover curves for 15 frames of set B (5-storey) and 15 frames of set D (9-storey), in terms of base shear, V, normalized by the base shear at the formation of the first plastic hinge, V_1, versus the roof drift ratio (roof drift normalized by total height). This ratio (V/V_1) is denoted as α_u/α_1 in EC8 and represents the over-strength of the frame due to redistribution of forces after the formation of the first plastic hinge. The blue dots in the plots of Fig. 3 correspond to the peak base shear (capping strength) and the red dots show the base shear for a 20% post-peak strength reduction, V_{80}. The period-based ductility, μ_T, defined by FEMA P695 [1] as the ratio of the displacement corresponding to V_{80} to the effective yield roof displacement, has been calculated in order to have a preliminary estimate of the inelastic drift capacity of the frames. The values of μ_T for Set B range from 8.9 up to 12.7, while for Set D the corresponding range is from 4.1 up to 7.5. It is worth noting that the global lateral strength can vary significantly depending on the structural configuration (selection of steel profiles), although all the MRFs are code-compliant; this is not unexpected in seismic design. Finally, from the plots in Fig. 3 it is observed that in the case of the 3-storey configurations, the “negative stiffness” region mostly initiates at global drift levels of approximately 5%, while for the 9-storey configurations, degradation (in the global sense) starts at drift levels of 2.5%-3%.

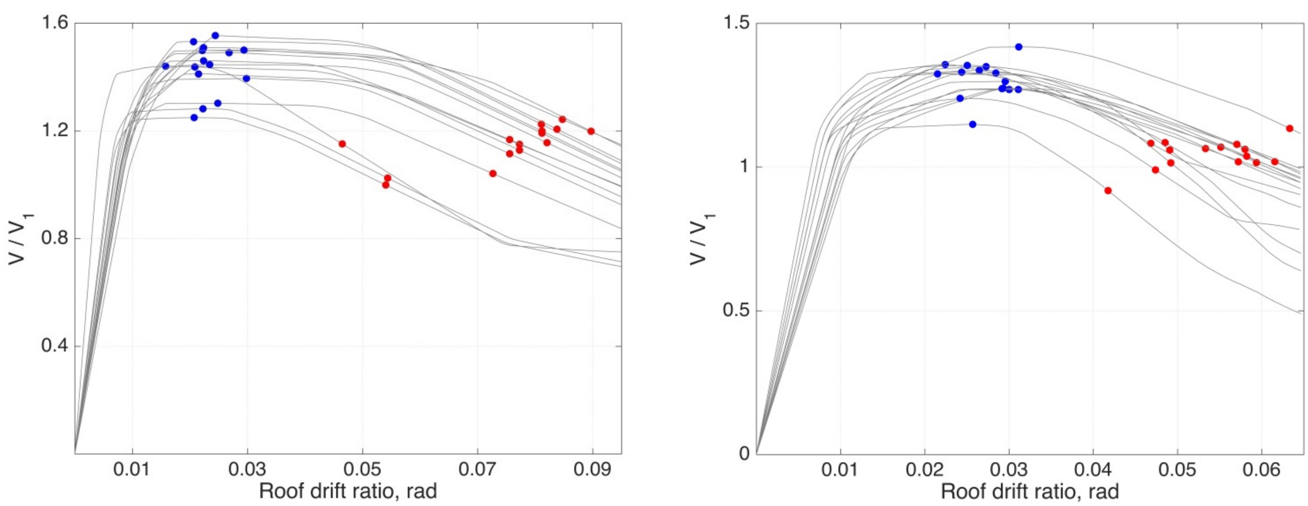

(a) (b)

Fig. 3 – Pushover analyses: base shear (V) normalized by base shear at first yield (V_1) vs. roof drift ratio for (a) 3-storey frames (set B), (b) 9-storey frames (set D). Blue dots correspond to peak global strength; red dots correspond to 20% post-peak strength reduction

4.3 Global drift demands from IDA

The pair of 3 and 5-storey low-rise frames (A03 and B15) exhibited mean IDA results virtually identical both for the lumped plasticity model (IMK) and the distributed plasticity model (Fibre). Fig. 4(a) presents the IDA curves for frame A03 in terms of maximum roof drift ratio as engineering demand parameter (EDP) and inelasticity levels (q') as intensity measure (IM). Consequently, independently of the modelling approach, the global drift demand (δ_{mod}) also reaches similar values. The trend of these values is presented in terms of the tuning ratio, which is defined as the fundamental period of the building, T_1, normalized by the mean period of the ground motion record, T_m, as shown in Fig. 5(a) for Frame A03. The δ_{mod} values for specimen A03 along the full T_1/T_m range (0.4-2.5) are steady at about 0.5-0.6 for all inelasticity levels. Meanwhile, Frame B15 is characterised by a constant δ_{mod} value around 0.7-0.9 for a T_1/T_m range of 0.5 to 3.5, for all values of q'. Finally, for the low-rise frames, the mean of the maximum roof drift ratios at the maximum intensity level considered ($q' = 6$) remains in the pre-capping region of the global pushover curves. This observation is consistent with previous studies indicating the relevance of cyclic degradation when the post-capping stiffness domain is attained in the response [20].

In the case of the 7 and 9-storey mid-rise frames (C08 and D01), the IDA results indicate stronger dependence on the modelling approach. Additionally, both frames exhibit structural collapse for certain NRHA analysis cases at the highest considered level of inelasticity ($q' = 6$) and for IMK modelling. Here, “collapse” is defined as large lateral displacement concentrated at one storey (usually at the base) with significant incursion in the negative stiffness slope beyond the capping corner in the global lateral capacity curve (pushover). Fig. 4(b) illustrates such collapse occurrences for Frame C08. Based on this, the incremental dynamic analysis for δ_{mod} was carried out up to an intensity level $q' = 5$, and the mean maximum roof drifts observed correspond to deformation levels before the capping (max. lateral strength) point in the corresponding monotonic pushover curve. However, at this inelasticity level ($q' = 5$), the effect of cyclic deterioration inherent in the IMK modelling approach can be observed in terms of larger maximum roof drifts, compared to the non-deteriorating case. From the estimation of mean δ_{mod} for low-rise Frame A03, presented in Fig. 5(a), it is obvious that the average trends of the global drift modification factor are practically identical for the degrading and the non-degrading case. On the other hand, from the estimation of δ_{mod} for mid-rise Frame C08, presented in Fig. 5(b), it is observed that the mean trend for the deteriorating frames (IMK model) is slightly above the respective trend for the non-deteriorating cases (Fibre model) in the central frequency region (tuning ratio of 2 to 3) but considerably larger in both the low and high frequency regions. Both cases exhibit the same shape and dependency on ground motion mean period. Although the data is presented for just one inelasticity level, a trend can be noted and an average difference of 20% can be roughly estimated for the δ_{mod} depending on the modelling approach.

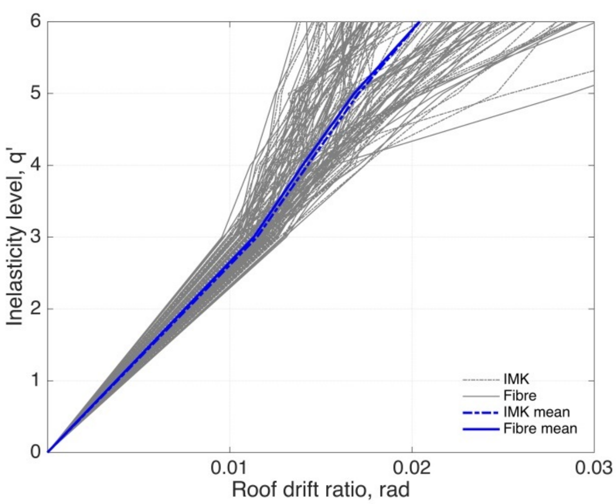

(a)

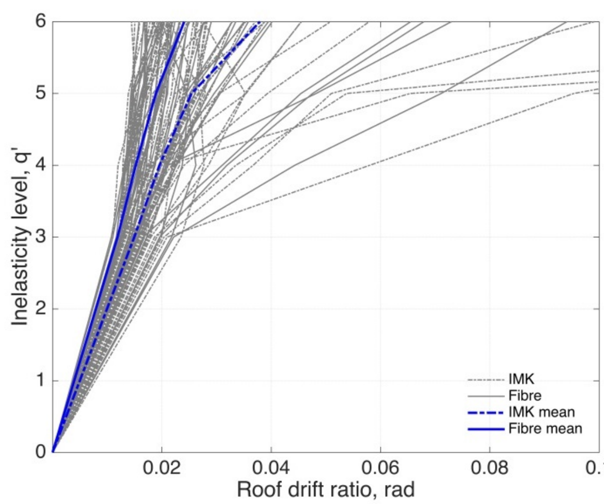

(b)

Fig. 4 – IDA curves: inelasticity level versus max roof drift ratio for (a) Frame A03 and (b) Frame C08

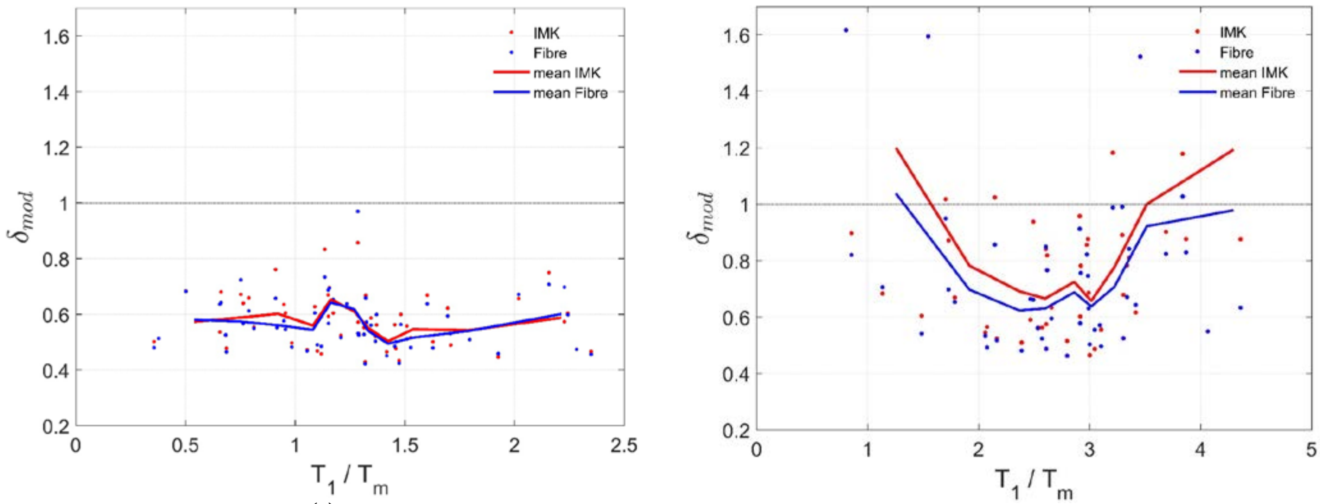

Fig. 5 – Global drift modification factor (δ_{mod}) as a function of T_1/T_m at $q' = 5$ for (a) Frame A03 and (b) Frame C08. Dots represent single analyses while lines depict average values.

4.4 Inter-storey drift demands from IDA

The results of the IDA were processed following a procedure similar to that described in the previous section in order to estimate the maximum drift modification factor, θ_{mod}. For the low-rise frames, the mean IDA curves for the maximum inter-storey drifts are essentially coincident as can be seen in Fig. 6(a) for Frame A03. Therefore, θ_{mod} for both modelling approaches is practically identical and does not seem to be affected by cyclic deterioration. The modification factor θ_{mod} reaches mean values from 0.5 to 0.7 in a range of tuned periods (T_1/T_m) of 0.5 to 2.5 for Frame A03 at all inelasticity levels considered. For its part, Frame B15 achieves θ_{mod} values around 0.8 to 1.0 at a range of tuned periods of 0.5 to 3.5 for all inelasticity levels. The estimation of θ_{mod} from IDA results for the Frame A03 is depicted in Fig. 7(a) for inelasticity level $q' = 5$ and, again, a non-T_m dependent behaviour can be observed over the range of tuning ratios considered. For this specific case the effect of cyclic deterioration is negligible in an average sense.

However, the results for the mid-rise Frames C08 and D01, consistently with the results obtained for δ_{mod}, show more clearly the effect of cyclic degradation on the structural response. The IDA curves in Fig. 6(b) and the corresponding estimates of θ_{mod} in Fig. 7(b) depict this effect for mid-rise Frame C08 where, at the lowest inelasticity level ($q' = 3$), the degrading IMK model reaches a 20% higher level of θ_{max} with respect to the non-degrading fibre model, which increases to 40% for $q' = 5$. As was the case with δ_{mod}, the increase in the values of θ_{mod} when deterioration is considered in the modelling is more evident for low (<2) and high (>3) values of the tuning ratio. The values obtained are consistent with the predictions made in previous studies [7], [8].

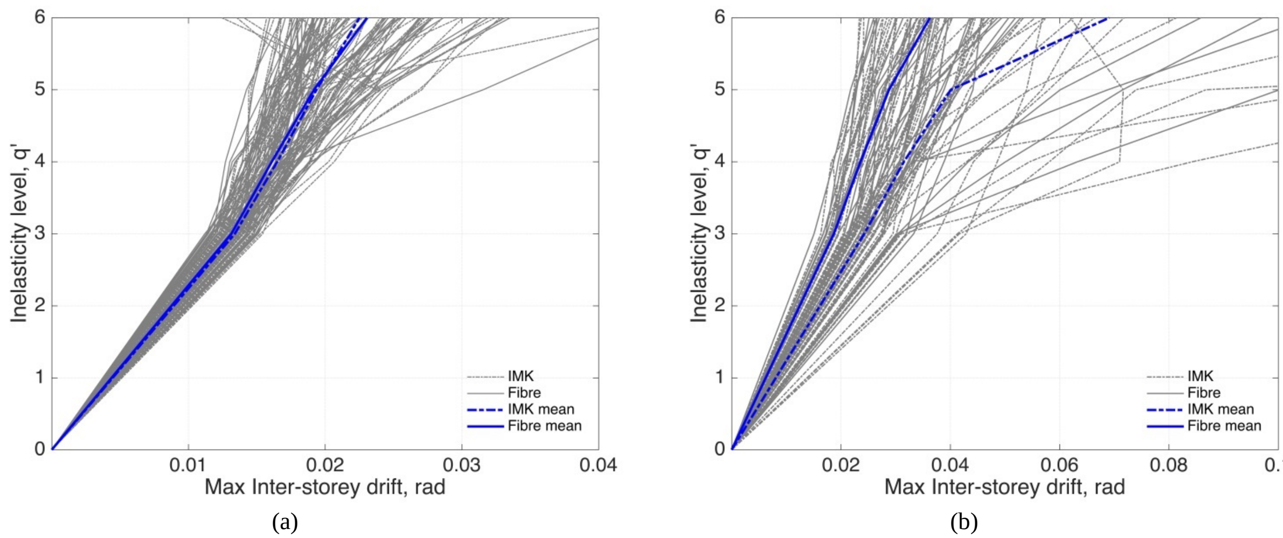

Fig. 6 – IDA curves: inelasticity level versus max. inter-storey drift ratio for (a) Frame A03 and (b) Frame C08

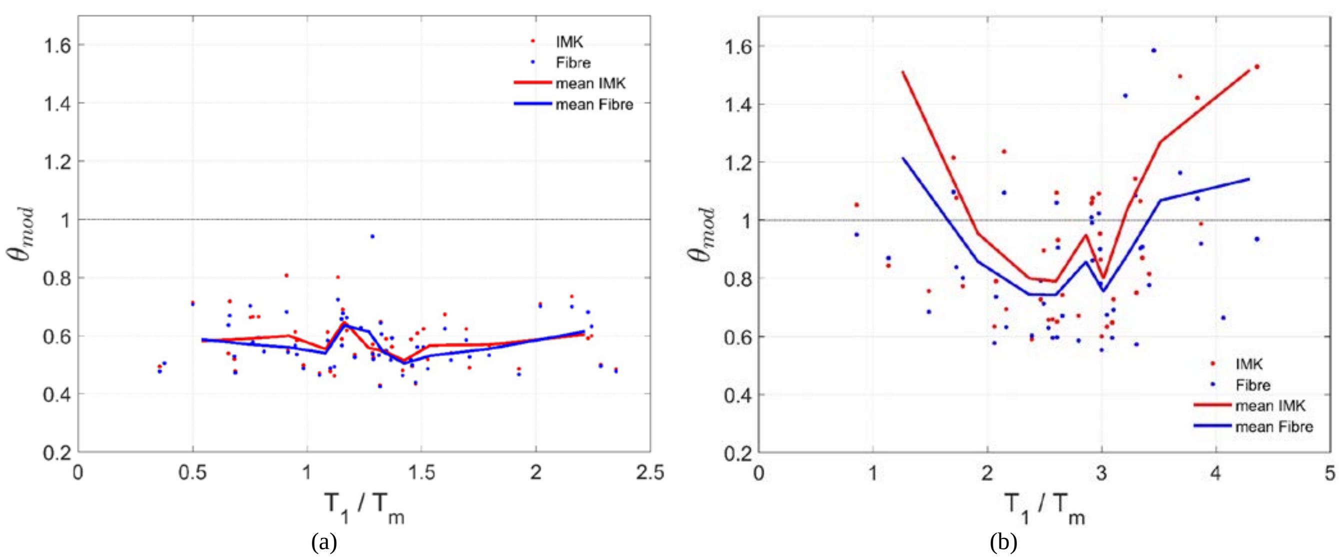

Fig. 7 – Max. inter-storey drift modification factor (θ_{mod}) as a function of T_1/T_m at $q' = 5$ for (a) Frame A03 and (b) Frame C08. Dots represent single analyses while lines depict average values.

5. Summary and conclusions

This paper investigated the effect of including cyclic degradation in numerical models, for typical steel moment resisting frames designed to EC8, in the estimation of peak inelastic seismic drift demands. To this end, non-linear static and dynamic analyses at various inelasticity levels were performed on a characteristic set of frames following: (i) the distributed plasticity modelling approach without deterioration and (ii) the concentrated (lumped) plasticity approach with cyclic degradation. The main findings of this ongoing research, for the set of frames and loading conditions considered, are as follows:

- For low-rise frames (3 and 5 storeys) the effect of cyclic degradation is negligible at all the inelasticity levels considered.

- For mid-rise frames (7 and 9 storeys) the effect of cyclic degradation may be relevant for certain structural cases that can reach the capping point for levels of inelasticity that are comparable with the EC8 seismic demand. These levels were determined to correspond to q' values between 4 and 5. For these cases, δ_{mod} can reach values up to 20% higher due to the cyclic degradation. The respective values for θ_{mod} can be up to 40% higher. The effect is more significant for low and high tuning ratios.
- With reference to the values obtained for δ_{mod} and θ_{mod} (lower than 1, on average) and considering that EC8 does not use any drift modification factor (i.e. uses the equal displacement rule), it can be postulated that EC8 is conservative in its prediction of inelastic seismic drifts, at least for the frame typologies considered in this paper.

Regarding modelling, when following the lumped plasticity approach, an adjustment is required in the local stiffness matrices of beam/column elements in order to properly simulate Rayleigh damping when significant inelasticity is present in the analysis. Moreover, the lumped plasticity method cannot directly take into account the axial force-bending moment interaction in the columns, which may be important especially for mid-rise frame typologies. In light of the preliminary results presented, it may be advisable to use distributed plasticity models whenever cyclic degradation is not expected to have a significant effect on the inelastic seismic response of the structure. Finally, this study also indicates that for specific structure and seismic loading combinations, structural collapse is reached at intensity levels q' comparable to the demands which the frames were designed to in the first place, which points towards the need for further assessment of codified design procedures.

6. Acknowledgements

The authors acknowledge the financial support of the “Consejo Nacional de Ciencia y Tecnología” (CONICYT, Chile) and the “Research Fund for Coal and Steel” of the European Community within the Project EQUALJOINTS: “European Prequalified Steel Joints”, Grant No RFCS-CT-2013-00021, for the work described in this study.

7. References

[1] FEMA (2009): Quantification of Building Seismic Performance Factors. *FEMA P695 Report*, Washington, DC.

[2] CEN (2004): Eurocode 8 (EC8): Design of structures for earthquake resistance—Part 1: General rules, seismic actions and rules for buildings. *EN 1998-1:2004*, European Committee for Standardisation, Brussels.

[3] Veletsos A, Newmark NM (1960): Effect of inelastic behavior on the response of simple systems to earthquake motions, *Proceedings of the 2nd World Conference on Earthquake Engineering*, pp. 895-912.

[4] Uang CM, Maarouf A (1994): Deflection amplification factor for seismic design provisions. *Journal of Structural Engineering*, 120(8), 2423-2436.

[5] Medina RA, Krawinkler H (2005): Evaluation of drift demands for the seismic performance assessment of frames. *Journal of Structural Engineering*, 131(7), 1003-1013.

[6] Pettinga JD, Priestley MN (2005): Dynamic behaviour of reinforced concrete frames designed with direct displacement-based design. *Journal of Earthquake Engineering*, 9(2), 309-330.

[7] Karavasilis TL, Bazeos N, Beskos DE (2008): Drift and ductility estimates in regular steel MRF subjected to ordinary ground motions: a design-oriented approach. *Earthquake Spectra*, 24(2), 431-451.

[8] Kumar M, Stafford PJ, Elghazouli AY (2013): Influence of ground motion characteristics on drift demands in steel moment frames designed to Eurocode 8. *Engineering Structures*, 52, 502-517.

[9] Málaga-Chuquitaype, C (2015): Estimation of peak displacements in steel structures through dimensional analysis and the efficiency of alternative ground-motion time and length scales. *Engineering Structures*, 101, 264-278.

[10] Chopra AK, McKenna F (2016): Modeling viscous damping in nonlinear response history analysis of buildings for earthquake excitation. *Earthquake Engineering & Structural Dynamics*, 45(2), 193-211.

[11] National Institute of Standards and Technology (NIST) (2010): Applicability of Nonlinear Multiple-Degree-of-Freedom Modeling for Design. *NIST Report GCR 10-917-9*, Gaithersburg, MD.

[12] ASCE/SEI (2010): Minimum design loads for buildings and other structures. *ASCE 7-10 Standard*, *American Society of Civil Engineers/Structural Engineering Institute*, Reston, VA.

[13] Lignos DG, Krawinkler H (2012): Development and utilization of structural component databases for performance-based earthquake engineering. *Journal of Structural Engineering*, 139(8), 1382-1394.

[14] D'Aniello M, Landolfo R, Piluso V, Rizzano G (2012): Ultimate behavior of steel beams under non-uniform bending. *Journal of Constructional Steel Research*, 78, 144-158.

[15] Lignos DG, Krawinkler H: (2010): Deterioration modeling of steel components in support of collapse prediction of steel moment frames under earthquake loading. *Journal of Structural Engineering*, 137(11), 1291-1302.

[16] Araújo M, Castro JM (2014): Deformation capacity of steel members. *Proceedings of EUROSTEEL 2014 Conference*, Naples, Italy.

[17] CEN (2005): Eurocode 3 (EC3): Design of steel structures–Part 1.1: General rules and rules for buildings. *EN 1993-1-1:2005*, European Committee for Standardization, Brussels.

[18] OpenSees (2016): *Open System for Earthquake Engineering Simulation*, *Ver. 2.5.0*, URL: opensees.berkeley.edu, as of May 15th, 2016.

[19] ATC (2010): Interim guidelines on modeling and acceptance criteria for seismic design and analysis of tall buildings. *PEER/ATC Technical Report 72-1*, Redwood City, California.

[20] Ibarra LF, Medina RA, Krawinkler H (2005): Hysteretic models that incorporate strength and stiffness deterioration. *Earthquake Engineering & Structural Dynamics*, 34(12), 1489-1511.

[21] Zareian F, Medina RA (2010): A practical method for proper modeling of structural damping in inelastic plane structural systems. *Computers & Structures*, 88(1), 45-53.

[22] Krawinkler H, Popov EP, Bertero VV (1975): Shear behavior of steel frame joints. *Journal of the Structural Division*, *ASCE*, 101(11), 2317-2336.

[23] Chiou B, Darragh R, Gregor, N, Silva W (2008): NGA project strong-motion database. *Earthquake Spectra*, 24(1), 23-44.

[24] Kumar M, Stafford PJ, Elghazouli AY (2013): Seismic shear demands in multi-storey steel frames designed to Eurocode 8. *Engineering Structures*, 52, 69-87.

[25] Elghazouli AY, Kumar M, Stafford PJ (2014): Prediction and Optimisation of Seismic Drift Demands incorporating Strong Motion Frequency Content. *Bulletin of Earthquake Engineering*, 12(1), 255-276.